Heterodyne Spectroscopy in the Thermal Infrared Region: A Window on Physics and Chemistry

Theodor Kostiuk[a],
NASA Goddard Space Flight Center, Code 693, Greenbelt MD 20771

ABSTRACT

The thermal infrared region contains molecular bands of many of the most important species in gaseous astronomical sources. True shapes and frequencies of emission and absorption spectral lines from these constituents of planetary and stellar atmospheres contain unique information on local temperature and abundance distribution, non-thermal effects, composition, local dynamics and winds. Heterodyne spectroscopy in the thermal infrared can remotely measure true line shapes in relatively cool and thin regions and enable the retrieval of detailed information about local physics and chemistry. The concept and techniques for heterodyne detection will be discussed including examples of thermal infrared photomixers and instrumentation used in studies of several astronomical sources. Use of heterodyne detection to study non-LTE phenomena, planetary aurora, minor planetary species and gas velocities (winds) will be discussed. A discussion of future technological developments and relation to space flight missions will be addressed.

INTRODUCTION

The thermal infrared region is an important region for remote studies of solar system, astrophysical and terrestrial sources. It contains spectral bands of many of the most important molecular and atomic species contained is gaseous sources. True shapes and frequencies of emission and absorption spectral lines from constituents of planetary and stellar atmospheres contain unique information on local physics and chemistry, including the temperature and abundance distribution, non-thermal effects, chemical composition, local dynamics and winds. Spectrometers capable of measuring spectra from remote thermal infrared sources require high sensitivity detectors and designs, which enable measurement of target spectra with sufficient spectral resolution to extract the desired physical and chemical parameters of the source. Infrared heterodyne spectroscopy provides the highest resolution, $\lambda/\Delta\lambda \geq 10^6$, high frequency specificity ($\geq 10^{-8}$), and sufficient sensitivity to uniquely measure gaseous constituents, non-thermal conditions, both thermal structure and species abundances, and gas velocities (winds) directly.

Infrared heterodyne detection is analogous to millimeter wave techniques. An infrared source is combined with a laser local oscillator, LO, and focused on an infrared photomixer, where the difference frequency between the source and laser frequencies is generated (Fig. 1). The resultant intermediate frequency, IF spectrum, is in the radio region of the electromagnetic spectrum and it preserves the intensity and spectral information of the infrared spectrum. It can be analyzed using radio techniques, e.g., filter banks, autocorrelators, or acousto-optic spectrometers, AOS's. These determine the absolute spectral resolution.

Heterodyne detection is a coherent technique and the detected electric field E_t is the sum of the of the electric fields of the source and laser local oscillator (Fig. 2). The detected power is proportional to E_t^2. The detected power consists of a DC term and the cross product, which is at the absolute difference frequency between the two incident signals, $|\omega_{lo} - \omega_s|$. The detected heterodyne signal is thus proportional to the product of the signal and laser power. At optimum operation the noise is dominated by the shot noise generated by the laser photons in the photomixer, shot-noise-limited (SNL) operation. The noise equivalent flux is then determined by the resolving element, B, by the integration time τ, and by the efficiency of the heterodyne system, the degradation factor Δ. This technique can also be used to build interferometers, preserving the phase information $\delta\phi$, as is done in the Berkeley Infrared Spatial Interferometer (ISI) at the Mount Wilson Observatory[1].

[a] E-mail: kostiuk@gsfc.nasa.gov

Figure 2 illustrates the sensitivity of heterodyne detection. The spectral intensity F is plotted vs. wavelength for various black body temperatures. These curves represent the photons/s/Hz detected by a heterodyne system with a diffraction limited etandue~λ^2. The noise equivalent flux, NEF, forΔ=10, B=25 MHz (0.00083 cm^{-1}), and τ=1hr is given by the horizontal dashed line. Target sources are indicated at their temperatures and at wavelengths of particular interest. The calculated signal to noise ratio is given on the right hand abscissa. As can be seen many sources are easily studied with the heterodyne technique (c.f. refs. 2, 3).

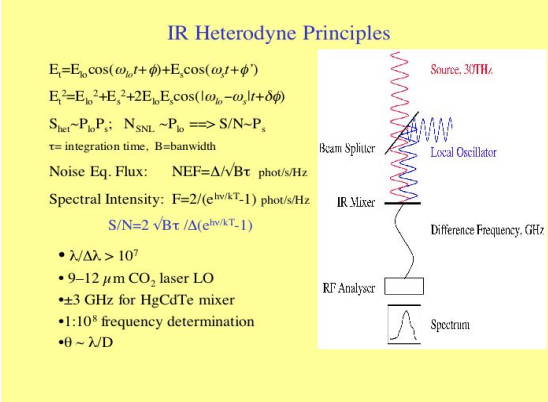

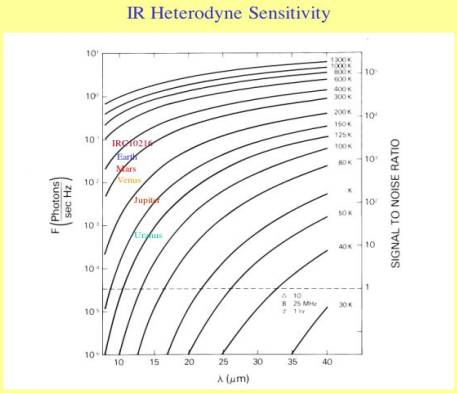

Fig.1 Principals of Infrared Heterodyne Detection *Fig. 2*

The critical components of an infrared heterodyne spectrometer are the laser local oscillator and detector/photomixer. Examples of measurements and scientific results that can be retrieved from infrared heterodyne spectroscopy will be presented, followed by a discussion of current infrared photomixer technology and some approaches for future device improvements.

INFRARED HETERODYNE SPECTROMETERS AND EXAMPLES OF MEASUREMENT RESULTS

Results using spectrometers developed at Goddard Space Flight Center: the GSFC Infrared Heterodyne Spectrometer (IRHS)[2,3] and a more recent Heterodyne Instrument for Planetary Wind and Composition (HIPWAC)[4]. HIPWAC is described in Figs. 3 and 4. The HIPWAC schematic in Fig. 3 illustrates the optical components including:

1) A dichroic mirror which splits most of the incident visible light into an optical guide system.
2) A calibration subsystem, consisting of an on-table chopper and a flip mirror, which can direct the output from a calibrated black body into the heterodyne detection system. The calibration subsystem can also be used to make laboratory measurements by inserting a gas cell into the black body optical beam.
3) Beam combining subsystem which matches and combines the signal beam and laser LO beams and focuses them onto a HgCdTe photodiode mixer. It consists of a signal beam collimating off axis parabola, OAP, a beam combining ZnSe beam splitter, BS, a on-mixer focusing OAP, and a laser beam attenuating, ATT, and beam expanding, BE, optics.
4) Dual CO_2 laser LO subsystem, consisting of two stabilized CO_2 lasers each of a different isotope, enabling nearly simultaneous operation at different wavelengths, e.g., near 10 μm with a normal isotope and near 12 μm with a carbon 14 CO_2 isotope.
5) RF Spectral line receiver, consisting of a 128 channel dual resolution (25MHz, and 5 MHz) RF Filter Bank.

Figure 4 shows HIPWAC and its electronics mounted on the NASA 3-meter Infrared Telescope Facility, IRTF on Mauna Kea, Hawaii. Most of the observational examples shown were measured at the IRTF.

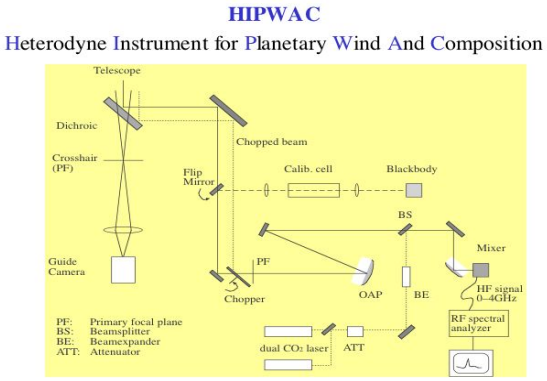

Fig.3. Schematic Layout

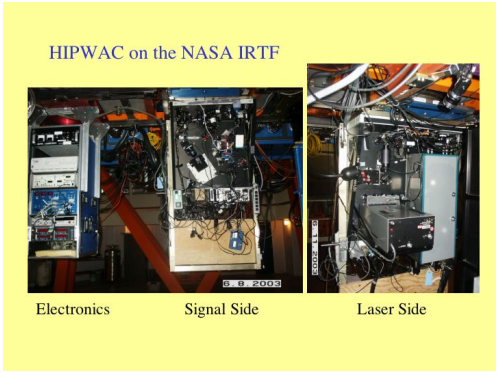

Fig. 4. HIPWAC at The IRTF

Jupiter - Comparison of spectral resolution. Figure 5 illustrates the advantage of heterodyne level spectral resolution. The bottom spectrum shows measurements of Jupiter's spectrum in the thermal infrared region with the Voyager Infrared Interferometer Spectrometer, IRIS[5], at a spectral resolution of 0.43 cm^{-1}. A broad spectrum displaying bands of molecular constituents of Jupiter's atmosphere near the north polar region is revealed. Analysis of the band of ethane near 12 µm probes lower stratospheric altitudes, pressures higher than 10 mbar. A Fourier transform spectrometer at 0.015 cm^{-1} resolution reveals individual sub-bands of ethane and isotopic ethane. This resolution probes higher in altitude, pressures greater than a few mbar. Infrared heterodyne resolution (0.00083 cm^{-1}) measures a single line shape in a sub-band thus probes even higher, pressures ≤1 mbar. All spectra permit retrieval of ethane abundance, stratospheric temperature information, however, is not independently retrievable with the lower resolution spectra. Resolved individual line shapes do permit retrieval information on both ethane abundance and temperature[6,7].

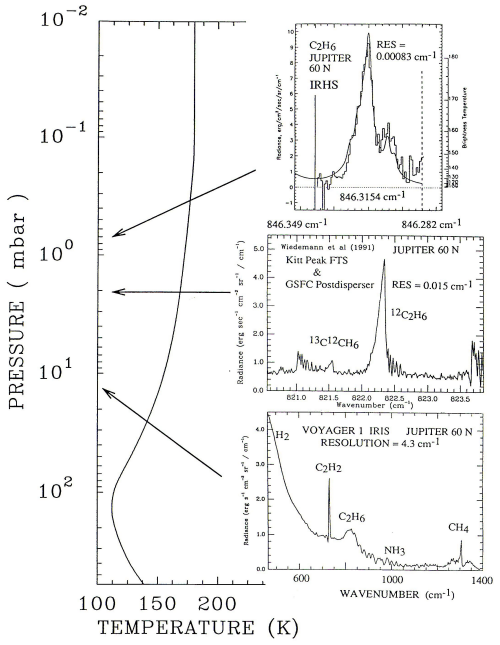

Fig. 5.

Mars CO_2 Absorption and Non-Thermal/Laser Emission: Figure 6 Illustrates how infrared heterodyne spectroscopy can detect and study unique phenomena on Mars. The spectra are a measurement of atmospheric absorption and emission lines of CO_2 in the atmosphere of Mars. The left spectrum was measured by HIPWAC at 25 MHz (0.00083 cm^{-1}) resolution over a 1.6 GHz (0.053 cm^{-1}) band. It shows the CO_2 absorption line formed in the lower atmosphere, below ~30 km altitude, and a core emission formed in the mesosphere, 50 – 80 km altitude. The absorption line requires very high resolution to even detect it. The emission core, shown in the right spectrum in Fig. 6 at 5 MHz resolution, can only be detected and measured at heterodyne resolving powers. It is generated under non-local thermodynamic (non-LTE) equilibrium conditions, at µbar pressures under pumping by near infrared solar radiation. These lines can be bright and have a naturally occurring lasing component[8,9]. They can be used as probes of the Mars mesosphere. Because they are formed in low-pressure regions they have Gaussian shapes. Their width measures the local kinetic temperature[10] and their integrated intensity their vibrational temperature. Their measured frequencies can be used to directly measure winds, as was done on Venus[11].

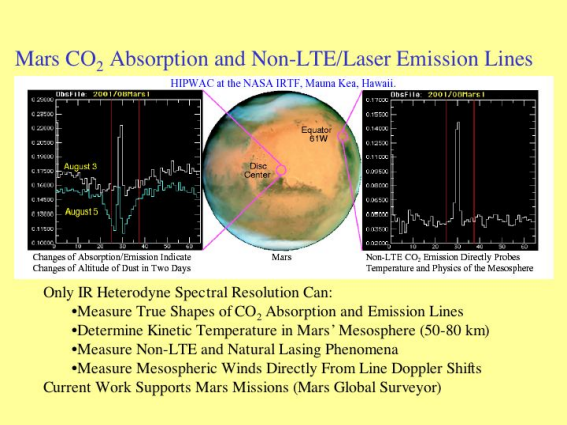

Fig. 6.

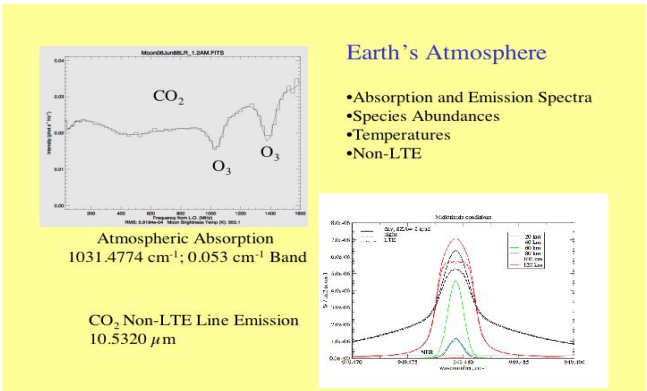

Fig. 7

Earth's Stratosphere - Constituent Abundance Profiles, Non-LTE: Figure 7 shows what can be measured in the Earth's stratosphere with thermal infrared heterodyne spectroscopy. Ozone[12], CO_2, ClO, and numerous minor constituents in the stratosphere can be measured. From Earth orbit non-LTE emission from numerous species including CO_2 (as on Mars and Venus) and ozone can be studied and the upper stratosphere and mesosphere probed. Calculations show significant non-LTE components possible as shown in the lower part of Fig. 7 (A. Kutepov, NRC/NASA GSFC, private communication, 2002).

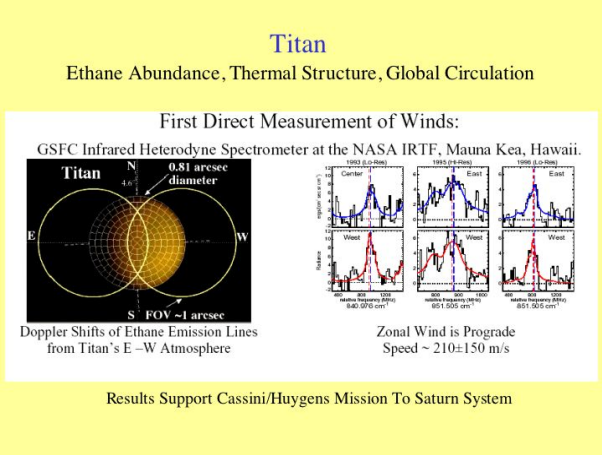

Fig. 8

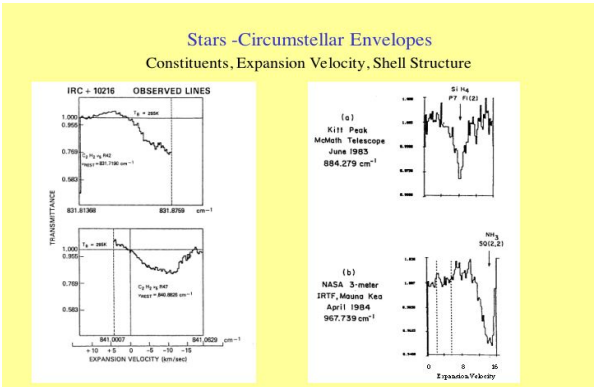

Fig. 9

Wind Measurements on Titan: Figure 8 shows results from direct measurements of the global circulation on Titan. Heterodyne resolution and high frequency determination enables direct measurement of gas velocities by measuring the Doppler shifts of individual spectral lines. This was done on Titan by measuring the difference in frequency of ethane line emission from east and west limbs of its disk[13]. The field of view of the IRHS is diffraction limited at the 3-meter IRTF, ~1 arcsec , and is shown in Figure 8. Resultant spectra were noisy due to the small portion of the Titan disk (~8.1 arcsec) that is in the measurements field-of-view. Global circulation was found to be prograde (east to west on the sky) with a speed 210 ± 150 m/s. Significant improvement in velocity uncertainty can be achieved with larger telescopes, e.g., 8-meter Subaru, whose field of view would be about 0.36 arcsec.

Circumstellar Envelopes – Composition and Shell Structure: Figure 10 illustrates species detectable with thermal infrared heterodyne techniques. Spectra of C_2H_2, NH_3, and SiH_4 are seen to probe different regions of the expanding shell of IRC10216. Acetylene is present throughout the stellar region and its line shape indicates shell structure, which can be compared to theoretical models.

HETERODYNE DETECTORS/PHOTOMIXERS

The key component of thermal infrared heterodyne detection is the photomixer, which determines the detection bandwidth and along with the system optical losses and laser power the system sensitivity. Conventional detectors can be photoconductors or photodiodes. Photodiodes (i.e., HgCdTe photodiodes) are the most commonly used

photomixers. In the conversion of incident photons to charge carriers only generation noise is present in photodiodes. In photoconductors both generation and recombination noise is present. This makes the photodiode inherently a factor of two more sensitive heterodyne detectors. However, photoconductors may have advantages in devices operating over a wider wavelength range. The principal goals of thermal infrared photomixer design are high heterodyne quantum efficiency, wide bandwidth of operation, and large wavelength coverage, particularly toward longer wavelengths (>12 μm).

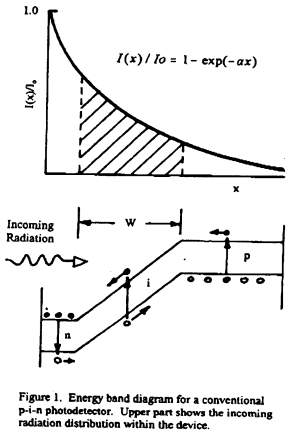

Fig. 10.Energy band diagram of Conventional p-I-n diode (Bratt, 2003)

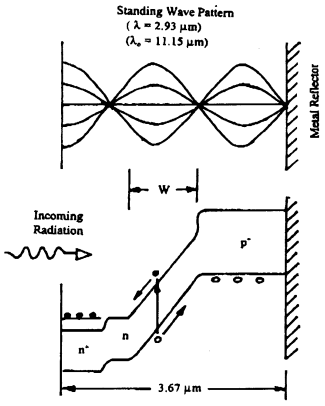

Fig. 11. Resonant optical cavity Energy levels and standing waves (Bratt, 2003)

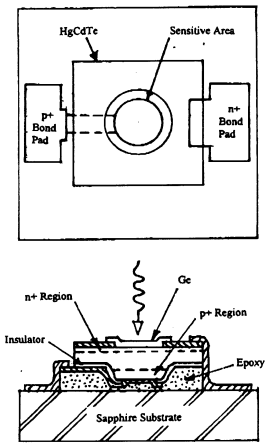

Fig. 12. ROC detector design (Bratt, 2003)

Figure 10 illustrates the energy level diagram for a conventional p-i-n photodiode (P. Bratt, Raytheon Vision Systems, private communication, 2003). Incoming radiation has only one path thought the material/junction, limiting the absorption and conversion efficiency and thus the heterodyne efficiency over wide bandwidths. If a resonant optical cavity, ROC, structure is used such as shown in Figs. 11 and 12, multiple passes are possible through the junction region, enhancing absorption of incident photons and thus the heterodyne quantum efficiency over a wide bandwidth (P. Bratt, Raytheon Vision Systems, private communication, 2003). These ROC devices are only tuned to relatively narrow wavelengths (Fig. 13) and, unlike with conventional diodes, multiple devices must be used for full wavelength coverage. Figure 14 compares the relative sensitivity and bandwidth of conventional HgCdTe GOF[14] and ROC photodiode mixers (Bratt, Raytheon Vision Systems, private communication, 2000).

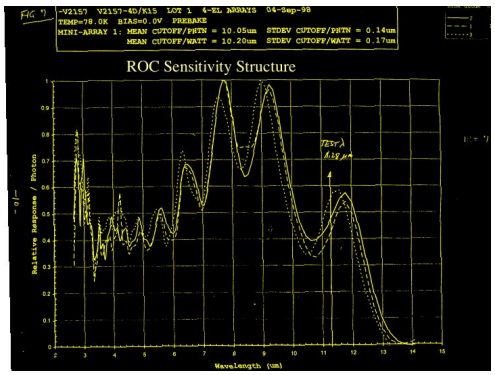

Fig. 13

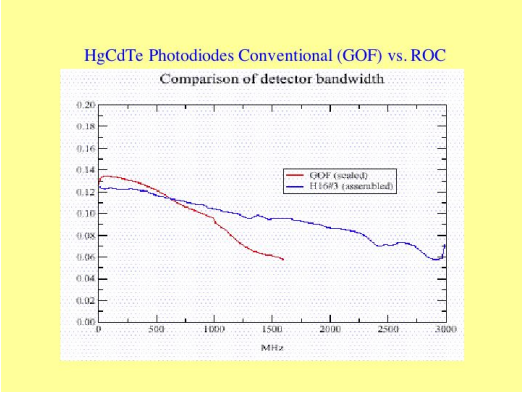

Fig. 14

Longer wavelength of operation can be achieved with photodiodes by material and doping adjustments and to a degree by cooling the device to colder temperatures, thereby reducing the energy gap, W. Results of such an approach by D. Spears (1987 and in Ref. 15) is shown in Fig. 15. This approach, however, limits the wavelengths to less than about 30 μm and bandwidths to about 500 MHz.

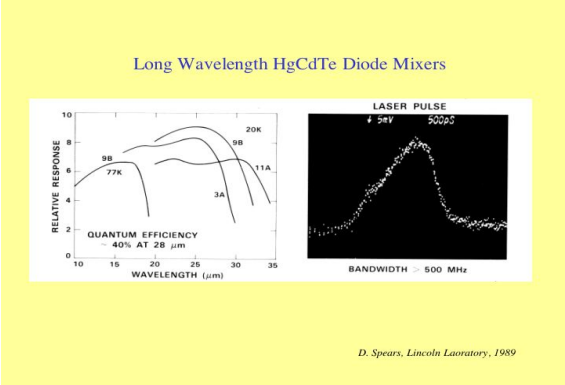

Fig. 15.

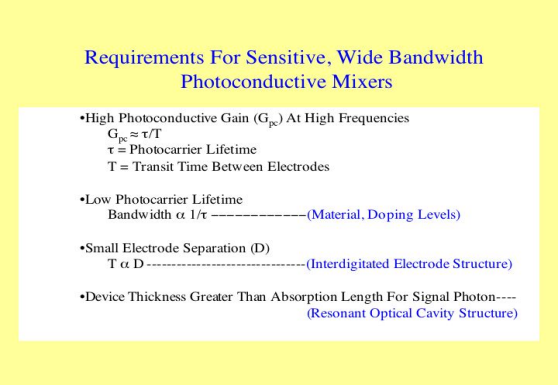

Table 1

Another approach for wide bandwidth, long wavelength photomixers which may yield devices operating to ~200 μm is interdigitated electrode ROC HgCdTe photoconductors. Requirements for sensitive and wide bandwidth photoconductive mixers are presented in Table 1. Devices must have high photoconductive gain at high frequencies, which means long carrier lifetime, τ, relative to the transit time between electrodes, T. If the transit time is short enough recombination is minimized and recombination noise becomes low or insignificant, approaching that of a photodiode. For wideband (fast) operation the photocarrier lifetime must be short. This is achieved by adjusting material composition and doping levels. The transit time between electrodes can be reduced by decreasing the distance, D, between them and, with an interdigitated structure, the multiple electrodes are able to effectively "sweep up" the photocarriers. For high quantum efficiency the effective device thickness must be greater than the absorption length. For thin devices, necessary for wide bandwidths, this can be accomplished with an ROC design as described previously. Figure 16 shows an image of ROC interdigitated HgCdTe photomixers at 28 μm. Figure 17 shows theoretical predictions for photodiode(dashed curve) and photoconductor (solid curve and band) long wavelength mixer performance[15]. Measured device performance is plotted as filled circles (photoconductor), triangles (photodiodes), and squares, GaAs Schottky diodes, for comparison to projected HgCdTe devices. ROC photoconductor mixers near 115 μm approaching the theoretical limit depicted here were fabricated[16].

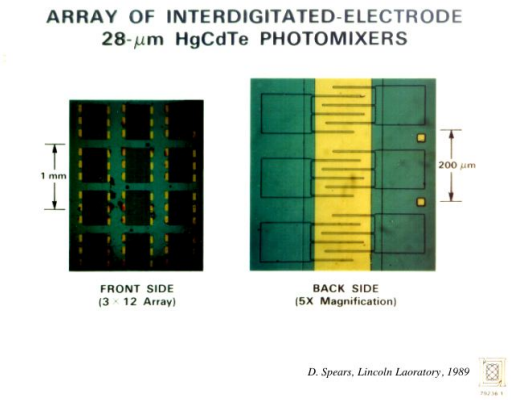

Fig.16

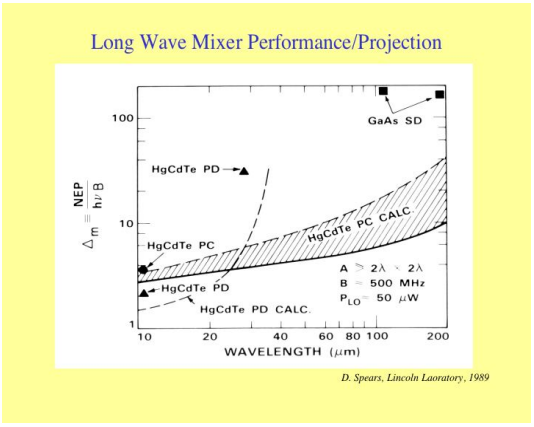

Fig. 17

FUTURE DEVELOPMENTS

Future improvements in photomixers includes development of truly operational devices in the 13-100 μm region with heterodyne quantum efficiency >60% and bandwidths≥4 GHz. Heterodyne mixer arrays need to be developed with sensitive and uniform device performance. The ROC interdigitated devices in Fig.16 are an example. Photodiodes have also been developed in small array formats (4-12 elements) but their uniformity in performance must be addressed. Other approaches that have not been addressed adequately are, hot bolometers and quantum well infrared photodetectors, QWIP's). QWIPS show promise and initial plans are underway to test existing devices for heterodyne performance and provide data for future development with photomixer performance as the focus.

REFERENCES

1. D. Hale, *A Thermal Infrared Heterodyne Receiver with Applications to Astronomy*, Proc. International Workshop on Thermal Detectors-TDW, Washington DC, USA, in press, 2003

2. T. Kostiuk, and M. J. Mumma, *Remote sensing by IR heterodyne spectroscopy*, Appl. Optics 17, 2644-2654, 1983.

3. T. Kostiuk, *Physics and chemistry of upper atmospheres of planets from infrared observations*, Infrared Phys. Technol. 35, 243–266, 1994.

4. F. Schmuelling, *et al*., *Heterodyne Instrument for Planetary Wind And Composition*, JQSRT, In Preparation, 2003.

5. R. A. Hanel, et al., Science, 204, 972, 1979.

6. T. A. Livengood, T. Kostiuk, F. Espenak, and J.J. Goldstein, *Temperature and abundances in the Jovian auroral stratosphere 1. Ethane as a probe of the millibar region*. JGR 98, 18813–18823, 1993.

7. T. Kostiuk, P. Romani, F. Espenak, T.A. Livengood, J.J. Goldstein, *Temperature and Abundances in the Jovian Auroral Stratosphere 2. Ethylene as a Probe of the Microbar Region*, JGR 98, 18823–18830, 1993.

8. M. J. Mumma, D. Buhl, G. Chin, D. Deming, F. Espenak, T. Kostiuk, D. Zipoy, *Discovery of natural gain amplification in the 10-micrometer carbon dioxide laser bands on Mars - A natural laser*, Science 212, 45–49, 1981.

9. D. Deming, F. Espenak, D. Jennings, T. Kostiuk, M. Mumma, D. Zipoy*, Observations of the 10-micron natural laser emission from the mesospheres of Mars and Venus*, Icarus 55, 347–355, 1983.

10. T. Livengood, T. Kostiuk, K. Fast, J. Annen, K., G. Sonnabend, T. Hewagama, *Meridional Mapping of Mesoapheric Temperatures from CO_2 Emission Lines Along the MGS Ground Track*, BAAS 35, 913, 2003.

11. J. J Goldstein, *et al.*, *Absolute Wind Velocities in the lower thermosphere of Venus using infrared heterodyne spectroscopy*, Icarus 94, 45–63, 1991.

12. K. Fast, T. Kostiuk, g. Sonnabend, T. Livengood, F. Espenak, J. Annen, M. F. A'Hearn, T Hewagama, *Peeking Through the Picket Fence: Observing Mars Ozone from Earth*, BAAS 35, 935, 2003.

13. Kostiuk *et al., Direct Measurement of Winds on Titan*, Geophys. Res. Lett. 28, 2361, 2001.

14. D.L. Spears*, Planar HgCdTe quadrantal heterodyne arrays with GHz response at 10.6 μm*, Infrared Phys 17, 5-8, 1977.

15. T. Kostiuk and D. Spears, *30 μm Heterodyne Receiver*, International Journal of Infrared and Millimeter Waves 8,1269-1279, 1987.

16. D. Spears, MIT Lincoln Laboratory, private communication, 1989.